European Review for Medical and Pharmacological Sciences 2018; 22: 810-819

Mitochondria-mediated disturbance of fatty acid metabolism in proximal tubule epithelial cells leads to renal interstitial fibrosis

W. SHEN, X.-X. JIANG, Y.-W. LI, Q. HE

Department of Nephrology, Zhejiang Provincial People's Hospital, People's Hospital of Hangzhou Medical College, Hangzhou, China

Abstract. – OBJECTIVE: To investigate the role of mitochondria-mediated fatty acid metabolism in proximal tubule cells in renal interstitial fibrosis.

MATERIALS AND METHODS: Intraperitoneal injection of folate was performed to induce renal interstitial fibrosis in mice. Polymerase chain reaction (PCR) was used to detect the expression of cytochrome c oxidase subunit IV (COX4IL) and phosphoenolpyruvate carboxykinase 1 (PCK1) in samples. Electron microscope was used to detect the activity of mitochondria. Serum creatinine and urea nitrogen were chosen as eval criteria for renal function. Western-blotti used to detect protein expression of cells. I nohistochemistry was used to test renal st ture and deposition of collagen.

RESULTS: In renal interstiti osis, m tochondria mediated the dy nd the promotion of tubulointerst fatty id metabolism. Besides, it coul o redu al interstitial fibrosis and alle he f tabolism of tubulointe ial

CONCLUSIONS: ochondr ysfunction induced fatty aci abolism is portant factor to promo ress of re interstitial fibrosis. Int ventio lated targets of fatty acid met lism is exp to become a new treatment renal interstiti osis.

Key W

Mi dri tty acid Proximal tubule epithelial cells, Re tial fib

Introduction

The incidence of chronic kidney disease ( ) is increasing year by year, accounting for of CKD patients in China[1]. Renal interstitial fibrosis is a common pathological manifestation of CKD resulted from various causes. Common unilateral ureteral ligation (UUL) mode chemia-re si model and the folic a l[2-4] are mo f acute kidney inju (AK d subsequent conversion to chronic kidney e e. Folic acid plays an imp role in the [5]. A large number o ic acid enter the bo y circulation to form ound folic a d crystallization, leading to e tubular n osis, and subsequently renal i titial fibr . Although it is well known tha ho t is the major site for fatty acid metab t is still uncertain whether mitochondria dysfunction will lead to fatty acid me- m and kidney damage. In addition, folic id o acts as important carbon unit carrier. Specifically, when the amount of folic acid in the circulation exceeds the physiological level, it will cause folic acid crystallization, which will further clog the tubules consequently leading to acute tubular damage and a remarkable decline in early renal function, especially for the first seven days. Renal dysfunction will persist for 30 days with gradual improvement, and eventually stabilization.

To verify the interplay among mitochondria, folic acid and renal interstitial fibrosis, first of all, it is important to establish a good model of renal interstitial fibrosis in our study. Common models of acute kidney injury (AKI) include unilateral ureteral ligation (UUL) model, ischemia-reperfusion model and the folic acid model[2-4]. AKI could subsequently be converted to CKD. Folic acid induced renal interstitial fibrosis model was applied in our study. Niclosamide is a salicylamide derivative that inhibits mitochondrial oxidative phosphorylation and reduces the ATP production of energy substance. It is certain that the exploration of the interplay among mitochondria, folic acid and renal interstitial fibrosis, will provide novel therapeutic options for renal interstitial fibrosis in the future.

Corresponding Author: Qiang He, MD; e-mail: swgongzuo@163.com

Materials and Methods

Mice and Animal Models

Male C57BL/6J mice weighing approximately 18-22 g were acquired from the Specific Pathogen-Free Laboratory Animal Center of Nanjing Medical University and maintained according to the Guidelines of the Institutional Animal Care and Use Committee at Nanjing Medical University. Folate (Sigma-Aldrich, St. Louis, MO, USA) was administered intraperitoneally at a dose of 300 mg/kg. Sham- intraperitoneally injected mice, were used as normal controls. The kidneys were harvested at 1, 7, 30, 90 days after they were intervened. A portion of the kidney was fixed in 10% phosphate-buffered formalin, followed by paraffin embedding for histological and immunohistochemical staining. Another portion was immediately frozen in Tissue-Tekoptimum cutting temperature compound (Tissue-Tek, Torrance, CA, USA) for cryosection. The remaining kidney tissue was snap-frozen in liquid nitrogen and stored at -80°C for extraction of RNA and protein. This study was approved by the [illegible] mal Ethics Committee of Nanjing Medic[illegible] versity, Animal Center.

Western-Blot Analysis

The kidneys were lysed [illegible] immunoprecipitation assay sol[illegible] cont[illegible]ng 1% NP40, 0.1% sodium do[illegible] sulfa[illegible] mL phenyl methane s[illegible]fony[illegible]e, 1% p[illegible] tease inhibitor coc[illegible]t, and [illegible]hosphatase I and II inhibitor[illegible]ktail (Sigm[illegible]rich, St. Louis, MO, U[illegible]e. The su[illegible]natants were collecte[illegible]fter c[illegible]fugation at 13,000 × g at 4°C[illegible] 30 min. [illegible]n concentration was det[illegible]ned by bicincho[illegible]c acid protein assay [illegible]A Ki[illegible]Pierce Thermo Fisher Scienti[illegible]Valth[illegible]MA, USA) according to the manufa[illegible]instru[illegible]ns. An equal amount [illegible]otein[illegible] loa[illegible] into 10% sodium do[illegible]ulfate[illegible]ylamide gel electrophoresis[illegible]DS-PAG[illegible] and transferred onto polyvin[illegible]difluoride (PVDF) membranes. The p[illegible]ry a[illegible]odies were as follows: anti-FN [illegible]ma-Aldrich, St. Louis, MO, USA), anti-α-S[illegible] (Sigma-Aldrich, St. Louis, MO, USA), anti[illegible]ulin (Sigma-Aldrich, St. Louis, MO, USA), anti-CPT-1 (Sigma-Aldrich, St. Louis, MO, USA) and tubulin (Sigma-Aldrich, St. Louis, MO, USA).

Quantitative Real-Time PCR (qRT-PCR)

Total RNA was extracted using TRIzol reagent (Invitrogen, Carlsbad, CA, USA) according to the manufacturer's instructions. cDNA was synthesized with 1 μg of total R[illegible] Tra Ace (Vazyme, Jiangning, Na[illegible]g, Chin[illegible] and oligo (dT) 12-18 primers. [illegible] expressio[illegible] was measured by Real-time P[illegible]say (Vazyme, Jiangning, Nanjing[illegible]China) [illegible]7300 Real-time PCR system[illegible]pplied Bi[illegible] Foster City, CA, USA[illegible]he rel[illegible]ive amo[illegible]f mRNA or gene to [illegible]nal c[illegible]ol was calculated using the eq[illegible]A[illegible]n whi[illegible]ACT = CT gene − CT [illegible]rol.

Immunoh[illegible]mical Sta[illegible]g

Kidne[illegible]ctio[illegible]3 μm thickness were fixed for 15 min in 4% p[illegible]rmaldehyde, followed by [illegible]bilization [illegible]0.2% Triton X-100 i[illegible]osphate-buffered sa[illegible]ne (PBS) for 5 min [illegible]oom temper[illegible]ure. After blocked with 2% [illegible]key serum [illegible]60 min, the slides were im[illegible]stained w[illegible]anti-FN (Sigma-Aldrich, St. Lo[illegible], anti-α-SMA (Sigma-Aldrich, St. Lo[illegible], USA), and collagen I (Sigma-Aldrich (St. Louis, MO, USA).

[illegible]ed Serum Creatinine, Urea Nitrogen and ATP

To detect creatinin, urea and ATP levels, Creatinine Assay kit (DIUR-500, BioAssay Systems, Hayward, CA, USA), urea Assay kit (DICT-500, BioAssay Systems, CA, USA) and ATP (EATP-100, BioAssay Systems, Hayward, CA, USA) were used according to the instruction.

Statistical Analysis

Western-blotting, RT-PCR, and immunohistochemical staining were all repeated at least three times independently. The histologic analysis and immunostaining, quantification were performed by using Image-Pro Plus 6.0 software (Media Cybernetics, Silver Springs, MD, USA). For Western-blot analysis, quantitation was performed by scanning and analyzing the intensity of the hybridization signals using NIH Imagine software. All data examined are presented as mean±SD. Statistical analysis of data was performed using the Sigma Stat Software (Jandel Scientific Software, San Rafael, CA, USA). Comparisons between groups were made using one-way ANOVA, followed by Student's *t*-test. $p<0.05$ was considered statistically significant.

Results

Folate-Induced Renal Fibrosis is in a Time-Dependent Manner

On the first day after intraperitoneal injection of 300 mg/kg.bw folic acid, the renal function of mice (serum creatinine and blood urea nitrogen) in the experimental group was significantly improved. Although mice in experimental group recovered gradually, the recover period was still longer than 30 days. In addition, the level of blood urea nitrogen at day 1, 7 and 30 were higher than those in the control group; the differences were statistically significant ($p<0.05$) (Figure 1A, B). At day 1, tubular dilatation was presented after folate injection, tubule epithelial cells became necrotic, and renal interstitial fibrosis started at day 7 (Figure 1C). Besides, a large amount of red collagen formed at day 30 (Figure 1C). Quantitative analysis showed that the Masson and collagen staining positive regions presented an increasing trend over time (Figure 1D, E).

Increased Expressions of Folic Acid Induced Renal Fibrosis Related Indi

Renal interstitial fibrosis is characteriz[ed] by inflammatory cell infiltration[7-9], accumula[tion] of extracellular matrix (ECM)[10,11], innate c[ell] lular activation, proliferation [and] henotyp[ic] loss. Fibroblasts are the maj[or] CM-producing cells that express α-SMA [and] othe[r] markers after activation[12]. Immu[no]stoch[emical] ning showed that the [expr]es[sion] SMA [and] collagen I in renal ti[ssue] increa[sed] significantly from day 1 to 30. [It] peaked at d[ay] α-SMA was mainly in t[he] interstitial [and] glomerular basement membr[ane] while the collagen I was in the [peri]tubuloin[terst]ial (Figure 2A). Western [blot] results showed [that] the expression of FN [and] α-SM[A] increased in a time-dependent [man]ner ($p<0.05$) with a peak value reached at [day] 7 (Figure 2C).

Dysfunction of Mitochondrial in Tubulointerstitial Fibrosis

To [find] out the effect of mitochondria dysfunction [on] tubulointerstitial fibrosis, the expression levels of COX4IL and PCK1 were determined. As shown in Figure 3A, the mRNA level of COX4IL was significantly reduced at day 1 and 7. At the same time, mRNA expression of PCK1, a regulator of the tricarboxylic acid cycle, was also significantly decreased (Figure 3B). Next, we evaluated if there is morphological change of mitochondria between experimental and control groups. SEM results showed that the number of mitochondria decreased sharply and the morphology [was] and fragmented in the acute phase, the number of mitochondria recovered at day 7, which was longer than that in the acute phase. However, there was still morphological abnormalities compared with the control group (Figure 3C).

Fatty acid Metabolism Disorder in Folic Acid-Induced Nephropathy Mode

Fatty acid metabolism is the main mode of energy supply in proximal tubular epithelial cells. The experimental results showed that the mRNA expression of key enzymes of fatty acid metabolism was decreased after injection of folic acid. A semi-quantitative analysis of the oil red positive region suggested that it was maximal at day 7 and still remained higher at day 30 compared to that of the control group (Figure 4A). Lipid deposition demonstrated lipid synthesis and catabolism were active. CPT-1a is a key enzyme which regulates the transport of fatty acids into the mitochondria; its decreased expression suggests a fatty acid transport disorder. Therefore, we measured the expression level of CPT-1a after folic acid injection in renal tissues. When renal tissue specimens were induced by folic acid for 30 days, the results revealed a significant decrease in the expression of CPT-1a (carnitine palmitoyl transferase 1a) (Figure 4B). The mRNA of CPT-1a in the total RNA of the tissue was also significantly decreased ($p<0.05$) (Figure 4C). The immunohistochemical staining indicated that expression of CPT-1a in the diseased part of the tissue was significantly decreased (Figure 4D). In addition, we found that the expression of carnitine acetyltransferase (Figure 4E) and ACOX1 (Acyl-CoA Oxidase1) was also decreased. Furthermore, the correlation between serum urea nitrogen level and mRNA expression of COX4IL in mitochondrial electron transport chain, and mRNA expression of fatty acid metabolism enzyme ACAD9 was further analyzed (Figure 4F). The results showed that the level of serum urea nitrogen was negatively correlated with mRNA expressions of COX4IL and ACAD9 (R^2 = 0.3985, 0.6213, respectively, $p<0.05$). The mRNA expression of COX4IL was positively correlated with the mRNA expression of ACAD9 (R^2 = 0.9453, $p<0.05$) (Figure 4G).

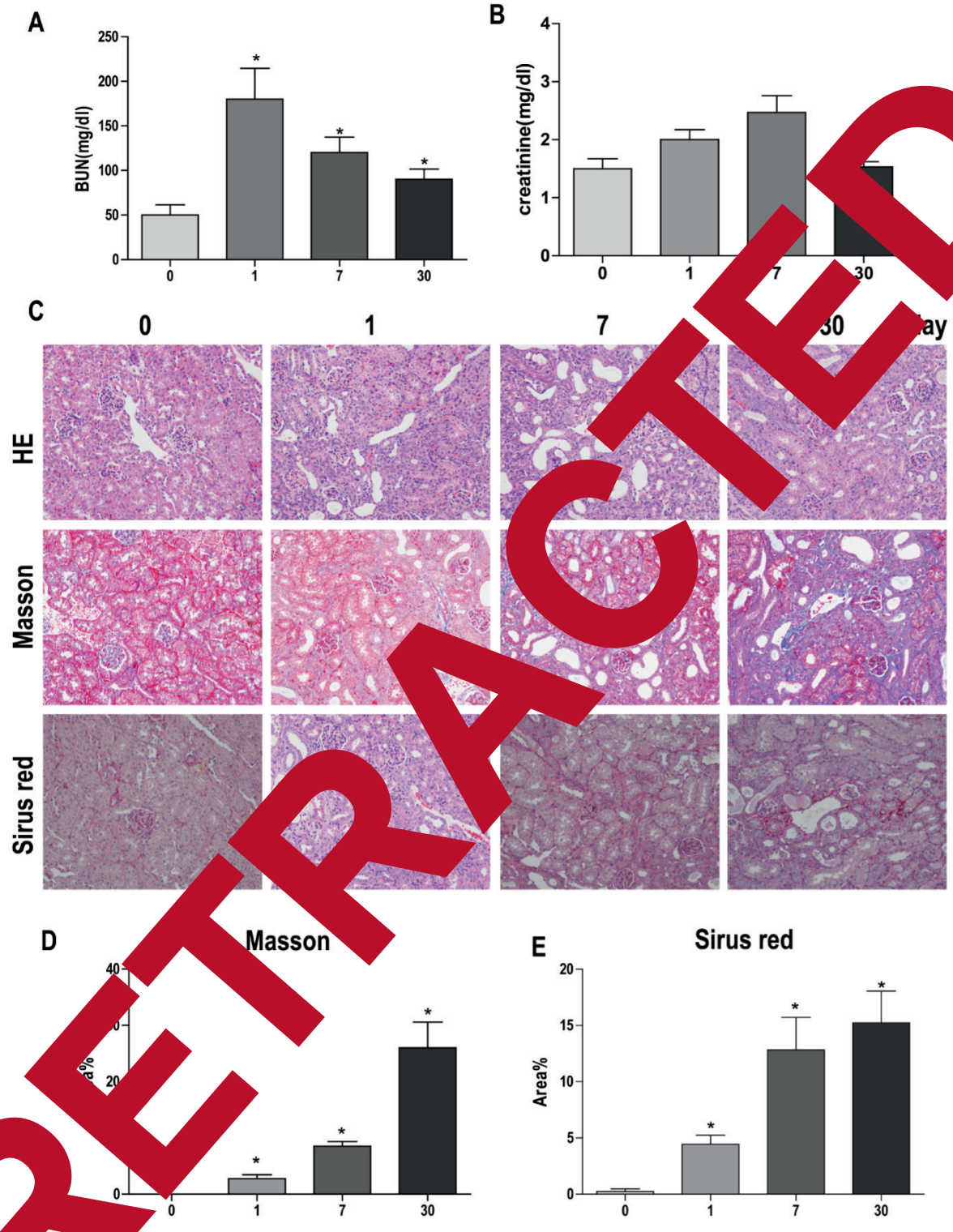

Figure 1. Folate induces renal function and kidney morphological changes in the animal model of renal fibrosis. ***(A)*** After a single intraperitoneal injection of 300 mg/kg.bw folic acid into B6 mice, blood was collected on day 0, 1, 7 and 30, and blood urea nitrogen was measured. *p<0.05 compared with that at day 0. (B) Results of determination of serum creatinine at day 0, 1, 7, 30 after single intraperitoneal injection of 300 mg/kg.bw folic acid injection, *p<0.05. ***(C)*** After a single intraperitoneal injection of 300 mg/kg.bw folic acid injection, pathological specimens of kidney were collected for day 0, 1, 7 and 30 day, and stained with HE, Masson and Sirus red (200×). ***(D)*** Semi-quantitative results of Masson stained in ***(C)***. *p<0.05. ***(E)*** Semi-quantitative results of Sirus red staining in ***(C)***. *p<0.05.

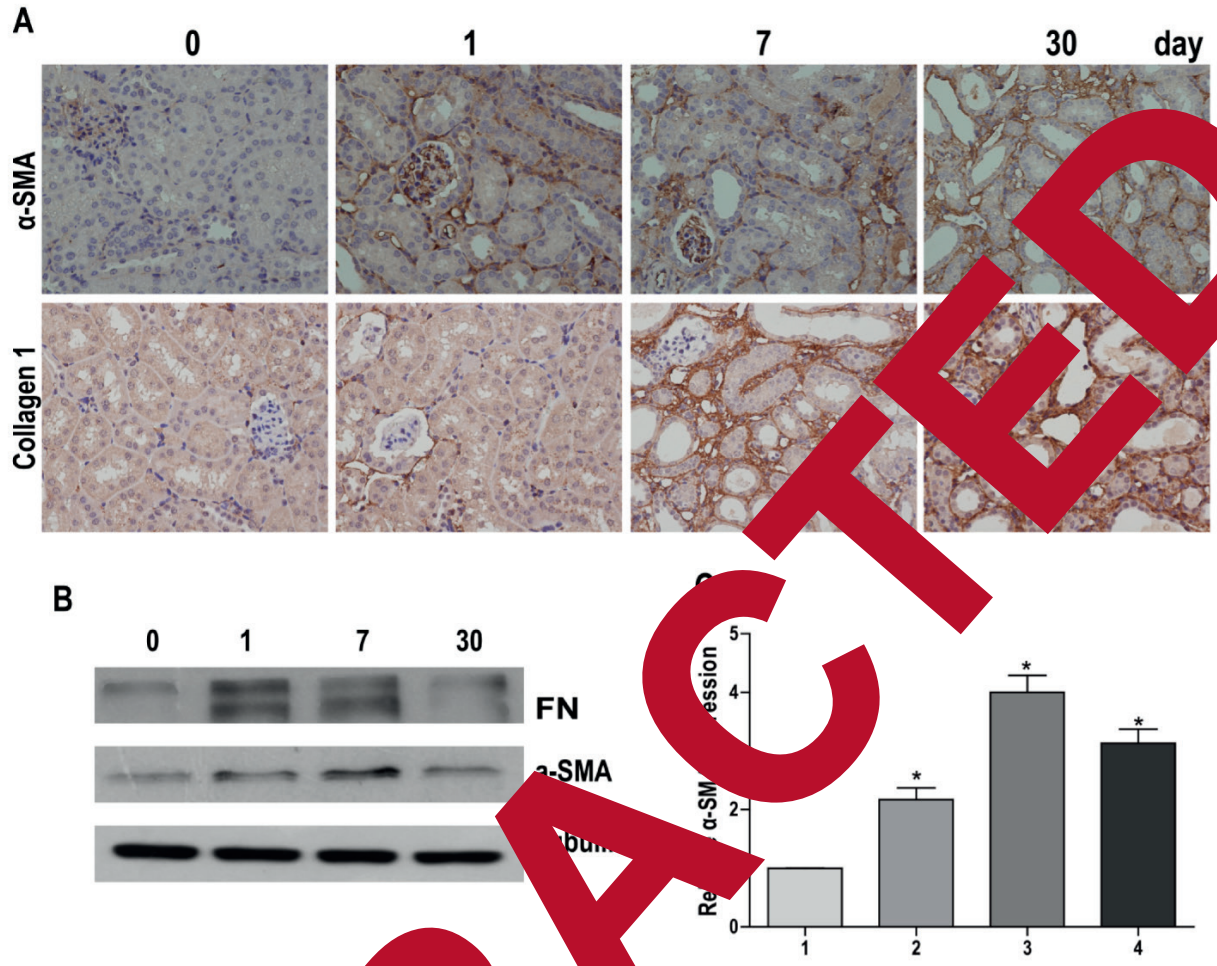

Figure 2. Folic acid induced renal ... sis m... of fibrosis ... ators in kidney expression. ***(A)*** After the mice were injected with folic acid, kidneys were col... at day ... 7 and 30, a... the immunohistochemical staining of α-SMA and Collagen I was performed (400×). ***(B)*** Wes... ot res... SMA in mouse kidney at day 0, 1, 7 and 30 after folic acid injection. ***(C)*** Semi-quantificatio... su... SMA ...). *p<0.05 compared to day 0.

Mitochon... al uncoup... Niclosa... e Ameliorates ... al Function and ... stitia...

F... s di... hydra...mine has a mitochondrial u... g effe... After intraperitoneal i... tion ... lic a... nto mice, niclosamide a... lly a... ered for one month. Our data ... monstra... that levels of serum creatini... urea nitrogen were significantly d... ased ... pared with the folate control ... up (Figure 5A, B). Meanwhile, the protein e... ssions of FN and α-SMA were decreased afte... atment with niclosamide (Figure 5C). Semi-quantitative analysis of α-SMA protein expression also showed significant differences between the treatment group and the folic acid group (Figure 5D), suggesting that niclosamide treatment can ameliorate renal interstitial fibrosis.

Niclosamide Treatment Ameliorates Fatty Acid Metabolism

The positive area of oil red staining in the folic acid treatment group was significantly decreased than that of the control group (Figure 6A). Western-blot results showed that niclosamide reversed the decrease in CPT-1a expression in the folic acid-induced renal fibrosis model (Figure 6B), and the mRNA expression of CPT-1a in total tissue RNA was also significantly increased compared to the folate group (Figure 6C). CRAT expression was also significantly incre-

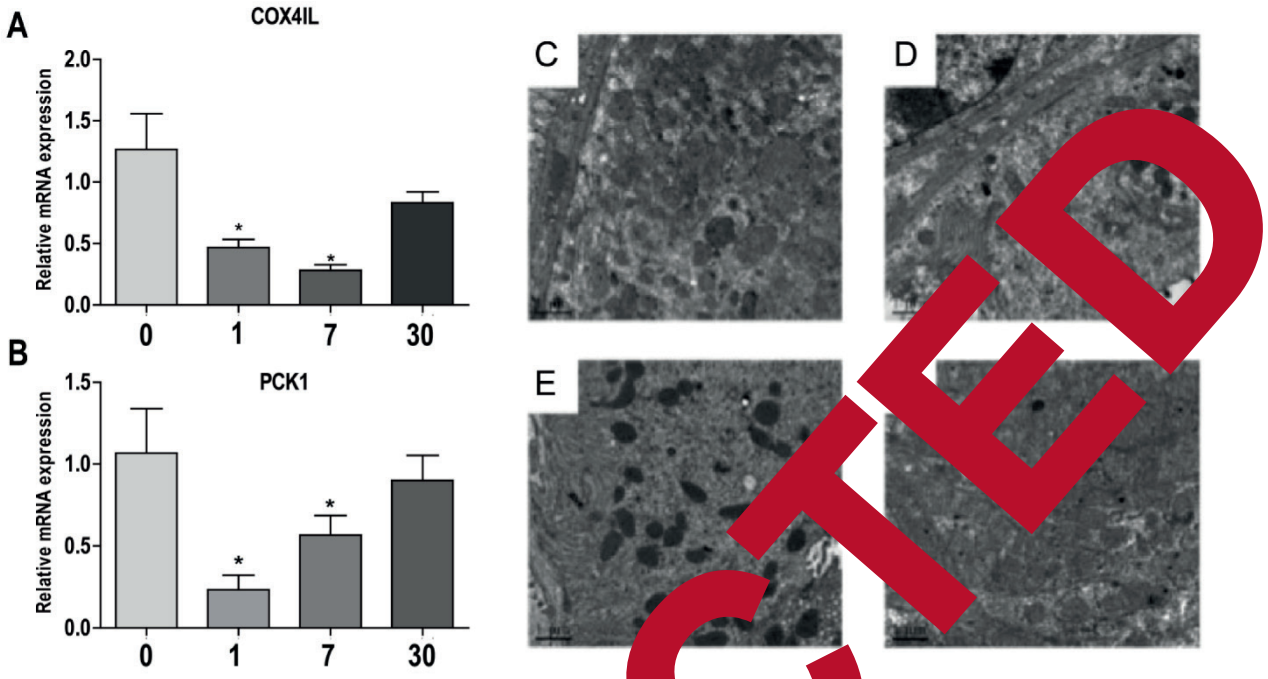

Figure 3. Changes in mitochondrial morphology and function in ...tic kidney ti... ***(A)*** Results of mRNA level of mitochondrial electron transport chain COX4IL in total RNA of mouse ... at day ... and 30. *$p<0.05$ compared with day 0. ***(B)*** Results of mRNA expression of PCK1, a key enzyme of the trica... ycle in total RNA of kidney of mice at day 0, 1, 7 and 30. *$p<0.05$ compared with day 0. ***(C...*** ... results of mitoch...ria after folic acid injection at ***(C)*** day 0, (D) day 1, (E) day 7, (F) day 30 (400×)**.**

ased (Figure 6D). Due to the r... of fatty acid metabolism, the activity ...sporter was restored and the fatty ...s were ...ansported into the mitochondri... oxida... energy supply, so tha... the ...n of lipid droplets was signif...tly red... Therefore, improvement of ... fibrosis by ...osamide can be speculat...

Niclosam... Affects Fa... Acid Oxidation Metabo... by Improving ...tochondrial Funct...

A... 0 da... oral administration of niclosamide ...ochon... morphology of kid... was ...red... the recovered amoun... mor... at of folic acid injection grou... $p<0.05$) ...igure 7A-E). Mitochondria are ...β-oxidation of fatty acids. A single b... inj... of folic acid may result in a re... ...tion in the number of kidney mitochondria a... ...nction loss, with a significant reduction in A... production. Interestingly, there was a significant increase in ATP production after niclosamide treatment (Figure 7F). Additionally, mitochondria are the main energy supply organelles in cells. A certain amount of energy is needed for mitochondrial activity. Therefore, we speculate that lack of intracellular energy during fibrosis may lead to the mitochondria dysfunction, retarded oxidation and decomposition. As shown in Figure 7G, fibrotic damage was observed after folic acid injection, whereas same amount of mitochondrial β-oxidation could not completely rescue the pheonotype. That being said, a slight recovery of fibrotic damage was observed, implying that the function of residual mitochondria in cells was activated, while the metabolic status of cells was not improved. After niclosamide decoupling, the ability of β-oxidation of mitochondrial fatty acids was fully activated, which accelerated the catabolism of lipolysis and reduced the deposition of intracellular lipids.

Discussion

Unlike UUL model and ischemia-reperfusion model, folic acid-induced renal fibrosis model does not require surgical procedures, and can

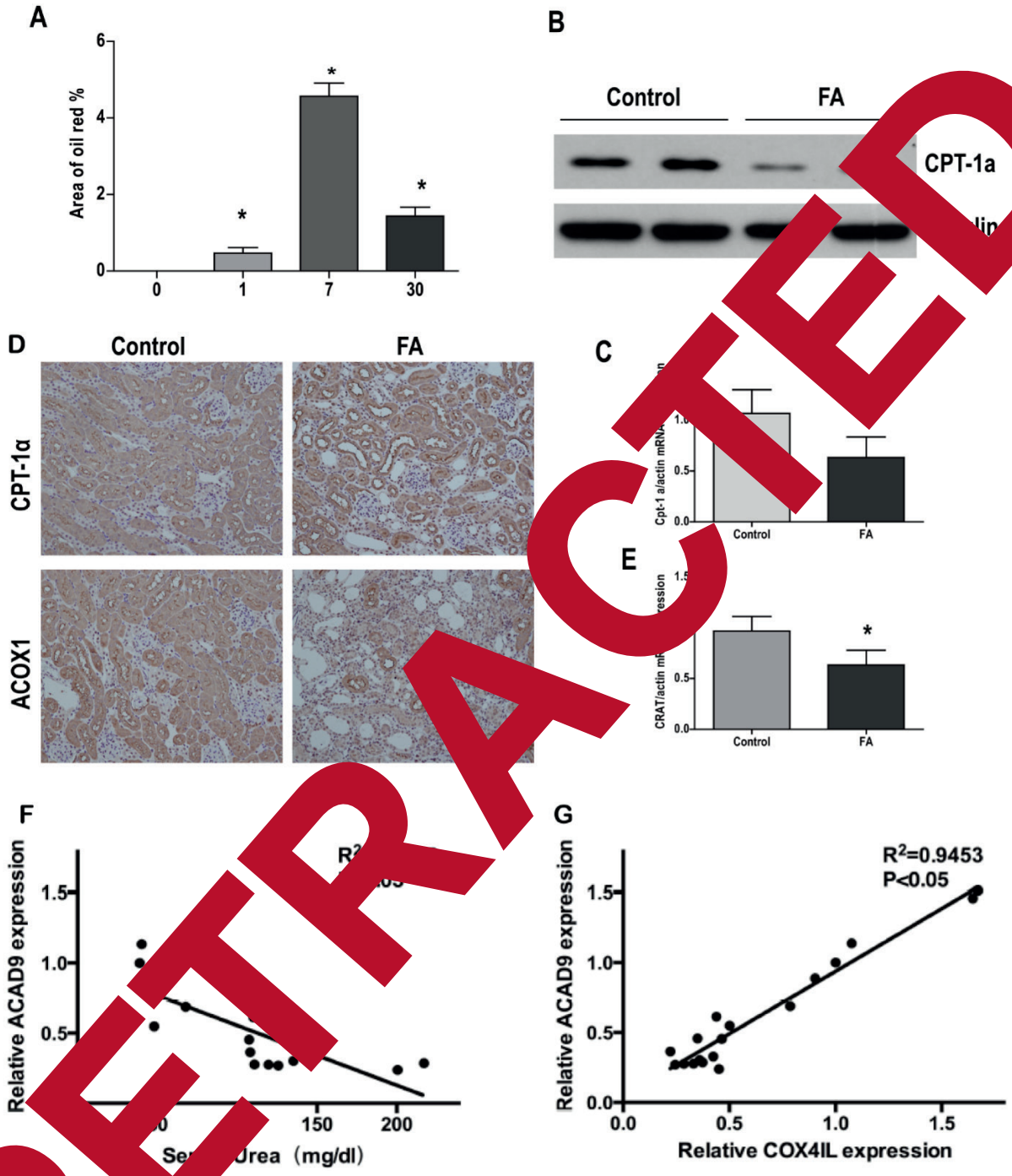

Figu Disord pression of fatty acid metabolism in fibrotic kidney tissue. ***(A)*** Semi-quantitative results of the areas staine sitive for o ed O in Figure 4 ***A-D***. The area on the vertical axis is the area marked by the oil red staining. *p<0.05 com 0. ***(B)*** Western-blot results of CPT-1a in renal tissue 30 days after folate injection. ***(C)*** mRNA expression o -1a NA of kidney tissue in control group and folic acid group 30 days after folate injection; *p<0.05 compared control group. ***(D)*** Immunohistochemical staining of CPT-1a and ACOX1 in renal tissue of control group and folic acid 30 days after folate injection (×200). ***(E)*** mRNA expression of CRAT in renal tissue of total RNA of control group and fo group 30 days after folate injection; *p<0.05 compared with control group. ***(F)*** Folic acid induced renal fibrosis model, co ation analysis results of serum level of urea nitrogen and expression of fatty acid metabolism key enzyme, ACAD9 mRNA. ***(G)*** Correlation analysis of folic acid induced renal fibrosis model, correlation analysis results of mRNA expressions of mitochondrial electron transport chain COX4IL and ACAD9, key enzymes of fatty acid metabolism.

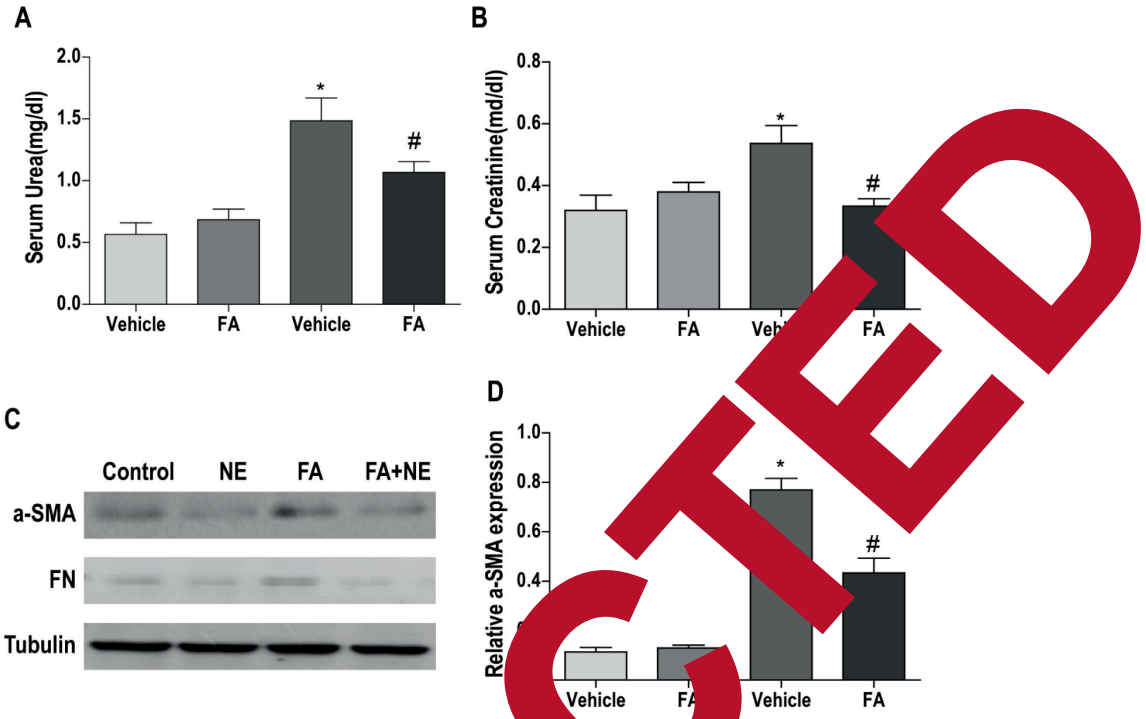

Figure 5. Niclosamide ameliorates renal function and tubulointers[illegible]brosis. *(*[illegible]*closamide treatment experiment was divided into four groups, blank control group (oral feeding of equal vol[illegible]ene glycol (solvent)), NE control group (oral feeding of equal volume of polyethylene glycol[illegible]ved niclosamide[illegible]acid group (fed with equal volume of solvent after folic acid injection) and folic acid treatm[illegible]ith equal volume of niclosamide after folic acid injection). *p<0.05 compared with control oral solvent group, [illegible]0.05[illegible]with folic acid oral solvent group. ***(B)*** Niclosamide treatment experiment, determination of serum creati[illegible]value[illegible]up. *p<0.05 compared with control oral solvent group; #p<0.05 compared with folic acid oral solvent gr[illegible]ter niclosamide treatment, Western-blot results of fibronectin α-SMA and FN in each group. ***(D)*** Semi-quantitative a[illegible]of α-SMA protein in (B), *p<0.05 compared with control oral solvent group; #p<0.05 compared with[illegible]l solvent g[illegible]

better simulate the natur[illegible]rse of[illegible]sis. Previous studies d[illegible]ons[illegible]t folic acid crystallization bloc[illegible]tubules[illegible]nal tubules after intraperiton[illegible]jection of[illegible]doses of folic acid. On t[illegible]and, large d[illegible]s of folic acid itself[illegible]e a ce[illegible]toxicity, which will damage th[illegible]bular epith[illegible]ells, promoting inflamm[illegible]y response and e[illegible]cellular matrix depos[illegible][5,6,14]. Our study demonstrated that folic[illegible]d ind[illegible]fibrosis model was divided into tw[illegible], acute[illegible]al injury and chronic [illegible]d fail[illegible]ge. [illegible]e renal injury appeared [illegible]d per[illegible]m day 1 to 7, which was follo[illegible]by ch[illegible]c renal failure stage. Mitocho[illegible]w an important role in regulating [illegible]y m[illegible]ism, while disorders of energy [illegible]abolism often promote disease progress[illegible]. This experiment demonstrated that in foli[illegible]d-induced renal fibrosis model, disturbances in mitochondrial structure and function led to activation of mitochondrial autophagy and subsequently apoptotic necrosis[16,17]. Fatty acids are the main energy-supplying substances in tubule epithelial cells[18]. When tubular epithelial cells undergo a stress response, their ability to metabolize fatty acids is reduced[19,20]. In this experiment, after folic acid led to renal interstitial fibrosis, the expression of key enzymes of fatty acid metabolism decreased, thereby exacerbating renal failure. There results suggested that mitochondrial damage induced fatty acid metabolism was the key factor to accelerate the progress of renal interstitial fibrosis. Mitochondria are coupled to the electron transport chain via oxidative phosphorylation to generate ATP, which can be destroyed by uncoupling agents[21-23]. Therefore, experimental mice were orally administrated with niclosamide for one month in our study, starting on the 8th day after folic acid injection. We found that fatty acid metabolism was increased whilst the degree of renal fibrosis was decreased, suggesting that improving fatty acid metabolism can reduce the renal interstitial fibrosis.

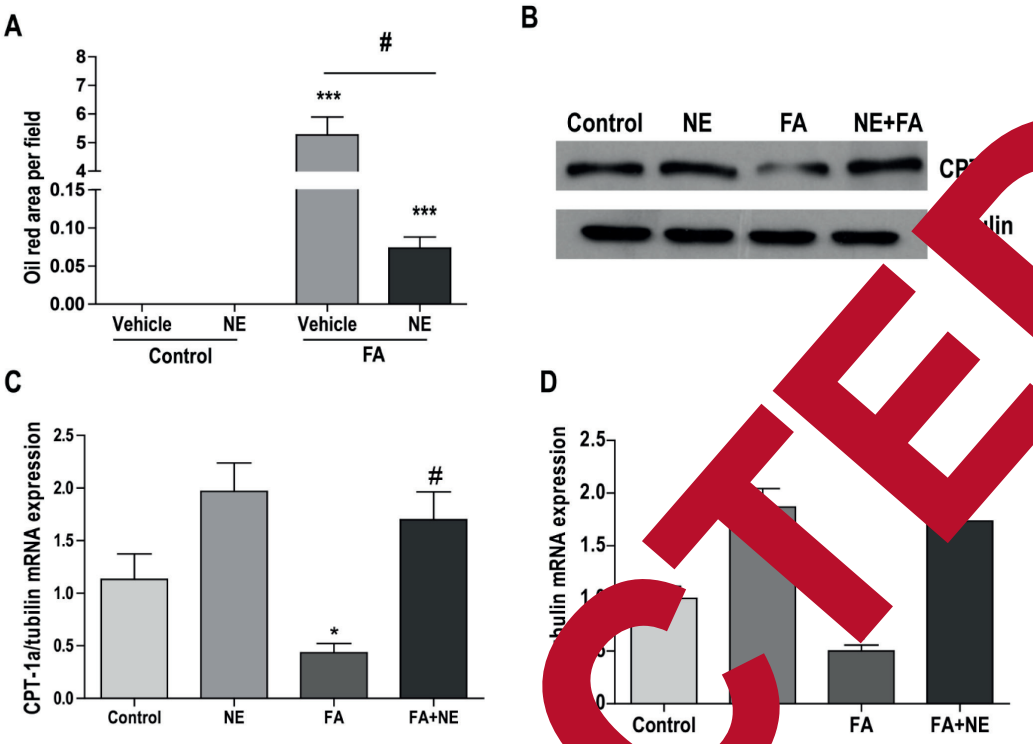

Figure 6. Niclosamide reduces tubulointerstitial fat deposition. ***(A)*** analysis of Oil red staining in picture A #$p<0.05$. ***(B)*** Western-blot of CPT-1a in each group. ***(C)*** The mRNA of each group. ***(D)*** The mRNA of CRAT in each group. *$p<0.05$ compared with control oral solvent group; #$p<0.05$ compared with folate oral solvent group.

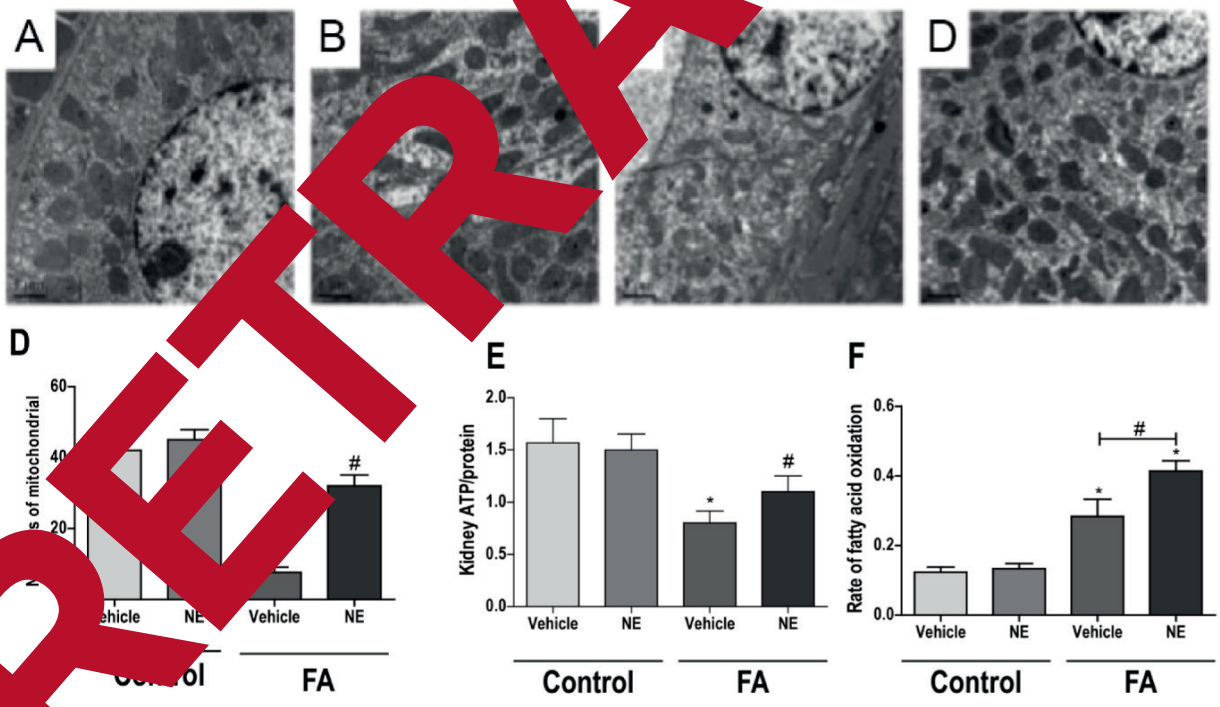

Figure 7. Niclosamide improves the function of mitochondria. (***A-D)*** Electron microscope results of mitochondri α (400×) ***(A)*** group, ***(B)*** Niclosamide control group, ***(C)*** Folate group, ***(D)*** Niclosamide treatment group. ***(E)*** Quantitative analysis of mitochondria; *$p<0.05$ compared with control oral solvent group; #$p<0.05$ compared with folate oral solvent group. ***(F)*** The number of ATP in Niclosamide group. *$p<0.05$ compared with control oral solvent group; #$p<0.05$ compared with folate oral solvent group. ***(G)*** The rate of fatty acid of mitochondrial oxidation in each group. *$p<0.05$ compared with control oral solvent group; #$p<0.05$ compared with folate oral solvent group.

Conclusions

In this study, folic acid-induced renal interstitial fibrosis was established as a model to investigate the relationship between renal interstitial fibrosis and mitochondrial fatty acid metabolism. Renal fatty acid metabolism was found impaired during renal interstitial fibrosis, whereas the uncoupler intervention and enhanced fatty acid metabolism can relieve tubule interstitial fibers. Mitochondrial damage caused by fatty acid metabolism is an important factor in promoting renal interstitial fibrosis. In this work, intervention of mitochondrial metabolism related targets was expected to become a new approach of treatment of renal interstitial fibrosis.

Conflict of Interest

The Authors declare that they have no conflict of interest.

References

1) Yano Y, Fujimoto S, Asahi K, Watanabe T. Prevalence of chronic kidney disease in China. Lanc 380: 213-214.

2) Correa RR, Pucci KR, Rocha LP, Pereira JC, Heli Machado JR, Rocha LB, Rodrigues AR, Gloria Guimaraes CS, Camara NO, Reis MA. Acute kidi injury and progression of ren after fet programming in the offsprin rats. Pe- diatr Res 2015; 77: 440-44

3) Gupta A, Puri V, Sharma S. Folic acute renal failure (ARF) b dant state. Exp Toxi athol : 225-232.

4) Vasko R, Xavier S J, Lin CH, B, Rabadi M, Maizel J, Tanok ang F, Cao J, rsky MS. Endothelial iency perpetr s nephrosclerosis thr gh dow tion of matrix metalloproteina 4: relevance sis of vascular senesc J Am Soc Nephro ; 25: 276-291.

5) Sh Li ZF, g YW, Liu SY, Wang WH. Effects c acid bined with vitamin B12 on DVT i nt homo teine cerebral infarction. Eur Pharm Sci 2017; 21: 2538-2544.

6) tos S, R J ga A, Largo R, Fernandez-Agul- Gazapo J, Esbrit P. Up-regulation of parathyroid hormo elated protein in folic acid-induced nal failure. Kidney Int 2001; 60: 982-995.

7) . Dissection of key events in tubular epithelial to myofibroblast transition and its implications in renal interstitial fibrosis. Am J Pathol ; 159: 1465-1475.

8) ujala PR, Sanati M, Jankowski J. Cellular and molecular mechanisms of chronic kidney disease with diabetes mellitus and cardiovascular diseases as its comorbidities. Front Immunol 2015; 6: 340.

9) Latchoumycandane C, Hanouneh M, Nagy LE, McIntyre TM. Inflammatory PAF receptor signaling initiates hedgehog signaling and kidney fibrogenesis during ethanol consumption. PLoS One 2015; 10: e145691.

10) Loeffler I, Wolf G. Epithelial-to-m l transition in diabetic nephropathy: Cells 2015; 4: 631-652.

11) Tang WB, Ling GH, Sun L, Zha hu X, Zhou X, Liu FY. Smad anchor for recept tion regulates high Glucose-Induc EMT dulation of smad2 and smad3 ties in r bul epithelial cells. Neph 015; 130: 213-

12) Duffield JS. Cellula molec echanis in kidney fibrosis. J vest 124: 2 9-2306.

13) Tao H, Zhang Zen an GL . Niclosamide eth mine-i mild chondrial uncouplin proves diab ms in mice. Nat Me 0: 1263-126

14) Li X, Qi ng X. 4-1BB-mediated signals confer protection t folic acid-induced nephro- Kidney Bloo s Res 2012; 36: 10-17.

15) o A, DelRaso NJ, Sc ger JJ, Chan VT. D-Serine exposure resulted in gene expression changes indicative of vation of fibrogenic pathways and down-regulat f energy metabolism and oxidati- stress res se. Toxicology 2008; 243: 177-192.

16) mirisa A, Kennedy DJ, Haller ST, Bu- iro JI, Malhotra D. Mitochondrial impairment in the five-sixth nephrectomy model of chronic renal failure: proteomic approach. BMC ol 2013; 14: 209.

17) Sansanwal P, Yen B, Gahl WA, Ma Y, Ying L, Wong LJ, Sarwal MM. Mitochondrial autophagy promotes cellular injury in nephropathic cystinosis. J Am Soc Nephrol 2010; 21: 272-283.

18) Kang HM, Ahn SH, Choi P, Ko YA, Han SH, Chinga F, Park AS, Tao J, Sharma K, Pullman J, Bottinger EP, Goldberg IJ, Susztak K. Defective fatty acid oxidation in renal tubular epithelial cells has a key role in kidney fibrosis development. Nat Med 2015; 21: 37-46.

19) Otto AM. Warburg effect(s)-a biographical sketch of Otto Warburg and his impacts on tumor metabolism. Cancer Metab 2016; 4: 5.

20) Lan R, Geng H, Singha PK, Saikumar P, Bottinger EP, Weinberg JM, Venkatachalam MA. Mitochondrial pathology and glycolytic shift during proximal tubule atrophy after ischemic AKI. J Am Soc Nephrol 2016; 27: 3356-3367.

21) Itami N, Shiratsuki S, Shirasuna K, Kuwayama T, Iwata H. Mitochondrial biogenesis and degradation are induced by CCCP treatment of porcine oocytes. Reproduction 2015; 150: 97-104.

22) Klotzsch E, Smorodchenko A, Lofler L, Moldzio R, Parkinson E, Schutz GJ, Pohl EE. Superresolution microscopy reveals spatial separation of UCP4 and F0F1-ATP synthase in neuronal mitochondria. Proc Natl Acad Sci U S A 2015; 112: 130-135.

23) Suzuki T, Kikuchi H, Ogura M, Homma MK, Oshima Y, Homma Y. Weight loss by Ppc-1, a novel small molecule mitochondrial uncoupler derived from slime mold. PLoS One 2015; 10: e117088.